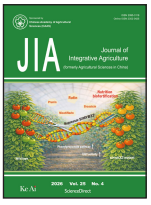
Journal of Integrative Agriculture 2026, 25(4): 1556–1565

Available online at ScienceDirect

Journal of Integrative Agriculture



RESEARCH ARTICLE

A *Fusarium pseudograminearum* secreted protein, Fp00392, is a major virulence factor during infection and identified as a PAMP

Qian Yang[1, 2#], Jing Wang[1, 2], Jixiang Sun[1, 2], Sijing Gao[1, 2], Hang Zheng[1, 2], Yuemin Pan[1, 2#]

[1] *Department of Plant Pathology, College of Plant Protection, Anhui Agricultural University, Hefei 230036, China*
[2] *Anhui Province Key Laboratory of Crop Integrated Pest Management, Anhui Agricultural University, Hefei 230036, China*

Highlights

- The *Fusarium pseudograminearum* secreted protein Fp00392 can activate the ROS burst, callose deposition, and the upregulation of defense-related genes in *Nicotiana benthamiana*.
- Fp00392 can induce plant immune response as a PAMP.
- Fp00392 promotes *F. pseudograminearum* infection as a virulence factor.

Abstract

As a main causal agent of wheat crown rot, *Fusarium pseudograminearum* secrets numerous proteins into the host during the infection process to regulate host immune responses and contribute to the virulence of *F. pseudograminearum*. In this study, the secreted protein Fp00392 from *F. pseudograminearum* was found to trigger cell death in *Nicotiana benthamiana*. Purified Fp00392 protein could activate the ROS burst, callose deposition, and the upregulation of defense-related genes in *N. benthamiana*. Moreover, the VIGS assay in *N. benthamiana* showed that Fp00392-triggered cell death is independent of BAK1 and SOBIR1. Furthermore, the transcript level of Fp00392 was significantly induced during *F. pseudograminearum* infection. Knockout of Fp00392 significantly attenuated the pathogenicity of *F. pseudograminearum* on wheat coleoptiles. Deletion of Fp00392 affected the sensitivity of *F. pseudograminearum* to H_2O_2 and Congo Red. Overall, these results indicate that Fp00392 can not only induce plant immune response as a PAMP, but it can also promote *F. pseudograminearum* infection as a virulence factor.

Keywords: *Fusarium pseudograminearum*, PAMP, cell death, virulence

1. Introduction

For survival in the natural environment, plants have evolved sophisticated defense mechanisms against the inevitable pathogens, including well-known PAMP-triggered immunity (PTI) and effector-triggered immunity (ETI). Among these mechanisms, PTI is the first level of basal immune response in plants, which is triggered by the mutual recognition of pathogen-associated molecular patterns (PAMPs) and pattern recognition receptors (PRRs) during pathogen infection (Jones and Dangl 2006). Typical PTI involves reactive oxygen species (ROS) burst, callose deposition, mitogen-activated protein kinase (MAPK) signaling and the upregulation of defense-related genes (Jones and Dangl 2006; Zipfel 2014).

PAMPs are evolutionarily conserved molecules in pathogens that can be peptidoglycans, cell wall degradation enzymes (CWDE), glycoproteins, chitins, or other secreted proteins (Liu B *et al.* 2012; Ranf *et al.* 2015). The well-characterized PAMPs include flagellin, peptidoglycan and elongation factor-Tu (EF-Tu) from bacteria (Felix *et al.* 1999; Kunze *et al.* 2004; Gust *et al.* 2007), as well as Pep-13 and glycoside hydrolase 12 protein XEG1 from oomycetes (Brunner 2014; Ma *et al.* 2015), and xylanase EIX, chitin and Ser-Thr-rich Glycosyl-phosphatidyl-inositol-anchored protein (SGP1) from fungi (Rotblat *et al.* 2002; Shinya *et al.* 2015; Song *et al.* 2021). Furthermore, the PRRs for detecting these PAMPs to active PTI have been identified gradually. For instance, flagellin and EF-Tu from bacteria are perceived by FLAGELLIN-SENSITIVE2 (FLS2) and EF-Tu receptor in *Arabidopsis thaliana*, respectively (Jones and Dangl 2006; Zipfel 2014); while XEG1 and EIX are perceived

Received 4 November 2024; Received in revised form 25 December 2024; Accepted 26 January 2025; Available online 18 February 2025
[#]Correspondence Yuemin Pan, E-mail: panyuemin2008@163.com; Qian Yang, E-mail: y.qwm@163.com

© 2026 CAAS. Publishing services by Elsevier B.V. on behalf of KeAi Communications Co. Ltd. This is an open access article under the CC BY-NC-ND license (http://creativecommons.org/licenses/by-nc-nd/4.0/). Peer review under responsibility of Editorial Board of *Journal of Integrative Agriculture*.
doi: 10.1016/j.jia.2025.02.030

by RXEG1 in *Nicotiana* and Eix2 in tomato, respectively (Ron and Avni 2004; Wang *et al.* 2018). Moreover, the distributions of different PAMPs among species vary. For example, glycoside hydrolase 12 protein XEG1 is widely distributed in oomycetes, fungi, and bacteria, whereas elicitin INF1 and SGP1 are specific to oomycetes and fungi, respectively (Kamoun *et al.* 1998; Ma *et al.* 2015; Song *et al.* 2021). In addition to these PAMPs with known conserved domains, some secreted proteins without known conserved domains have been identified as PAMPs that can activate the plant innate immune response, such as VmE02 from *Valsa mali* and PeSy1 from *Saccharothrix yanglingensis* (Nie *et al.* 2019; Wang *et al.* 2023). Nevertheless, only a few PAMPs from fungi that are perceived by plants to activate the innate immune response have been discovered.

Fusarium pseudograminearum is one of the main causal agents of wheat crown rot, which is one of the most devastating diseases in wheat and has caused large-scale losses in global food production (Akinsanmi *et al.* 2004). This pathogen can attack seeds in the early stage of wheat growth or subcrown internodes and spikes at the seedling stages, resulting in seed rot, the browning of subcrown internodes and white heads, respectively (Kazan and Gardiner 2018). In addition, *F. pseudograminearum* produces numerous toxins and secondary metabolites during infection, such as type-B trichothecene DON (3-acetyl- and 15-acetyl-deoxynivalenol, 3A-DON and 15A-DON) and nivalenol (NIV), which pose potential threats to food safety (Monds *et al.* 2005; Chakraborty *et al.* 2006; Obanor and Chakraborty 2014). This disease caused by *F. pseudograminearum* has continued to spread in many wheat-growing regions of the world (Kazan *et al.* 2018). For instance, first found in China in 2012, the disease caused by *F. pseudograminearum* had been reported in many provinces such as Hebei and Anhui (Li *et al.* 2012; Xu *et al.* 2015; Zhang *et al.* 2015; Ji *et al.* 2016). Given the continuing spread of the disease, investigating various aspects of the disease is particularly important, including the mechanism underlying plant–*F. pseudograminearum* interactions, which may guide the establishment of new strategies for the prevention and control of wheat crown rot.

In this study, we identified a PAMP from *F. pseudograminearum*, Fp00392, that triggers cell death in *N. benthamiana*. Fp00392 is homologous to VmE02 from *Valsa mali*, Fg02685 from *F. graminearum* and BFJ71_g10980 from *F. oxysporum*, which were reported previously (Nie *et al.* 2019; Xu *et al.* 2022) and are widely conserved in fungi. Fp00392 can activate the ROS burst, callose deposition, and the upregulation of defense-related genes in *N. benthamiana*. In addition, Fp00392-triggered cell death is independent of BAK1 and SOBIR1. Further analyses showed that Fp00392 is required for the virulence of *F. pseudograminearum* in wheat. The identification and functional characterization of Fp00392 are important for our understanding of how Fp00392 regulates the plant immune response and contributes to the virulence of *F. pseudograminearum* in wheat.

2. Materials and methods

2.1. Strains and culture conditions

The virulent *F. pseudograminearum* isolate used in this study, HNAY190416, was isolated by researchers in Anhui Academy of Agricultural Sciences from wheat that originated in Anyang, China. Wild-type *F. pseudograminearum* isolate HNAY190416 was routinely cultured on potato dextrose agar (PDA) medium at 25°C. To collect conidia, several mycelial plugs from PDA medium were cultured in carboxymethyl cellulose (CMC) liquid medium at 25°C for 3–5 days. A final concentration of either 0.5 mmol L^{-1} H_2O_2, 0.7 mol L^{-1} NaCl or 150 μg mL^{-1} Congo Red was added to the PDA for determining stress responses.

2.2. VIVE assay

The virus-induced virulence effector (VIVE) assay was performed according to the methods described previously (Shi *et al.* 2020). The full lengths of the 20 candidate effectors were amplified from *F. pseudograminearum* isolate HNAY190416 cDNA with specific primers (Appendix A) and inserted into pGR107 to construct 20 PVX-effector plasmids. *Agrobacterium tumefaciens* carrying the PVX-effector construct were infiltrated into 2-week-old *N. benthamiana* seedlings. Symptoms were monitored and recorded at about 3 weeks after infiltration.

2.3. RNA extraction and analyses of transcript levels

Total RNA was extracted using the Quick RNA Isolation Kit (Huayueyang Biotechnology, China). About 3 μg of the total extracted RNA was used for first strand cDNA synthesis with the HiScript II 1st Strand cDNA Synthesis Kit (Vazyme, China). The 2×S6 Universal SYBR qPCR Mix (EnzyArtisan, China) was used for the qRT-PCR assay. The primers used in the qRT-PCR assay are listed in Appendix A. Real-time PCR data were analyzed by the comparative $2^{-\Delta\Delta CT}$ method to quantify relative gene expression (Livak and Schmittgen 2001).

2.4. Yeast signal sequence trap system

To verify the function of the signal peptide of Fp00392, a yeast signal sequence trap system was designed as described previously (Yin *et al.* 2018). The predicted signal peptide of Fp00392 was cloned into the vector pSUC2 and transformed into yeast strain YTK12. The positive transformants screened on CMD-W medium (0.67% yeast N base without amino acids, 0.075% W dropout supplement, 2% sucrose, 0.1% glucose, and 2% agar) were incubated in CMD-W liquid medium for subsequent detection based on secreted invertase enzymatic activity. The invertase enzymatic activity was detected by the reduction of TTC to insoluble red TPF according to the methods described previously.

2.5. Subcellular localization analysis

To determine the subcellular localization of Fp00392, Fp00392 with or without the signal peptide was cloned into the vector pCAMBIA1302 to generate pCAMBIA1302:Fp00392-GFP and pCAMBIA1302:Fp00392Δsp-GFP, respectively. Strains of *A. tumefaciens* GV3101 carrying the above vectors were resuspended in infiltration buffer (10 mmol L^{-1} $MgCl_2$, 10 mmol L^{-1} MES pH 5.7, and 200 μmol L^{-1} acetosyringone)

and infiltrated into *N. benthamiana* leaves. At 48 h after agroinfiltration in *N. benthamiana* leaves, GFP fluorescence was observed under a confocal microscope with excitation at wavelength 488 nm. For plasmolysis, the infiltrated *N. benthamiana* leaves were detached and soaked in 0.8 mol L^{-1} sorbitol for 20 min.

2.6. Generation of Fp00392 deletion mutants and complementation strains

The *F. pseudograminearum* protoplasts were obtained and PEG-mediated fungal transformation was performed according to the methods described previously (Liu *et al.* 2013; Kang *et al.* 2023). For generating *Fp00392* deletion mutants, the upstream and downstream flanking sequences of *Fp00392* were amplified and fused to the hygromycin resistance gene *Hph* by overlapping PCR with the primers listed in Appendix A. The resulting PCR products were transformed into *F. pseudograminearum* protoplasts through the PEG-mediated transformation method. The *Fp00392* deletion mutants were screened using medium containing hygromycin (400 μg mL^{-1}) and a PCR assay with four sets of primers listed in Appendix A. Finally, Southern blotting was performed to verify the knockout of *Fp00392*. The 938 bp downstream segment of the Fp0392 coding region was amplified using primer Fp00392probe-F/R and labelled as the hybridization probe using the Digoxigenin (DIG) High Prime DNA Labeling and Detection Starter Kit I according to the manufacturer's instructions (Roche Applied Science, Germany). The genomic DNA was digested using *Bam*HI and *Kpn*I, and after blotting two bands of approximately 1.3 and 3.4 kb were observed in the wild type and mutant, respectively.

For generating complementation strains, the *A. tumefaciens*-mediated transformation method was used. The full-length Fp00392 gene with its native promoter was amplified and inserted into the vector pCETNS4, which was then transformed into *A. tumefaciens* strain AGL-1. Subsequently, *A. tumefaciens* containing the construct was mixed and co-incubated with conidia of Fp00392 deletion mutants on a nitrocellulose membrane, which was placed on an induction medium containing acetosyringone (200 μmol L^{-1}) at 28°C. After 2 days, the nitrocellulose membrane was transferred onto PDA plates containing cefotaxime (100 μg mL^{-1}) and geneticin (200 mg mL^{-1}) for screening the positive complementation strains, which were finally identified by PCR.

2.7. Infection assays with wheat seedlings

Infection assays with wheat seedlings were performed as described previously (Zhang *et al.* 2012). Briefly, fresh conidia of wild-type strain HNAY190416, deletion mutants and complemented transformants of Fp00392 were collected from cultures in CMC liquid medium at 25°C for 3–5 days and resuspended to 10^5 spores mL^{-1} in sterile double-distilled water (DDW). Subsequently, the top 1 to 2 mm sections of 3-day-old wheat coleoptiles were detached, and then the wound sites of the wheat coleoptiles were inoculated with 2 μL of the fresh resuspended conidium. The inoculated wheat coleoptiles were then maintained under suitable conditions for about 10 days when the phenotypes of wheat crown rot were photographed. Finally, the photographed wheat coleoptiles were collected to extract total DNA and further measure the biomass ratio of wheat and *F. pseudograminearum* by qRT-PCR using primers FpTubulin-F/R and TaEF-qRT-F/R.

2.8. Translocation assay of Fp00392 in wheat

The coding sequence of Fp00392 with the *F. pseudograminearum EF-1α* promoter was amplified and inserted into the pCETNS4-derived vector, which contained a fusion fragment of the red fluorescence gene mCherry and a nuclear localization signal (NLS), to generate the Fp00392-mCherry-NLS construct. Then, that construct was transformed into the wild-type strain HNAY190416 *via* the above-mentioned *A. tumefaciens*-mediated transformation method. Subsequently, the positive transformants were used to inoculate wheat coleoptiles according to the above-mentioned infection assays with wheat seedlings. At 72 h post inoculation, the mCherry signals in wheat tissues were observed under a confocal microscope.

2.9. VIGS in *N. benthamiana*

For the VIGS assay in *N. benthamiana*, the target genes were cloned into vector pTRV2 to generate pTRV2-gene constructs. Plasmids pTRV1 and pTRV2-gene were introduced into *A. tumefaciens* strain GV3101. The *A. tumefaciens* cultures carrying pTRV2-gene constructs and pTRV1 were resuspended in infiltration buffer (10 mmol L^{-1} $MgCl_2$, 10 mmol L^{-1} MES pH 5.7, and 200 μmol L^{-1} acetosyringone) to a final OD_{600} of 1.0, and then mixed in a 1:1 ratio to infiltrate into two primary leaves of four-leaf-stage *N. benthamiana* seedlings. pTRV2:PDS was used as a control to evaluate the efficiency of the VIGS system, whereas TRV:GFP was used as a negative control. The silencing efficiencies of the target genes were assessed using quantitative real-time PCR (qRT-PCR).

2.10. *In vitro* expression and purification of Fp00392

Fp00392 without the signal peptide was cloned into vector pET-32a(+), and the construct was introduced into *E. coli* BL21. Target protein Fp00392 was induced by 0.5 mmol L^{-1} isopropyl β-D-thiogalactopyranoside for 12 h at 16°C. At 12 h, the BL21 cells were collected and resuspended in phosphate-buffered saline, followed by comminution with an ultrasonic crusher. Subsequently, the supernatant from the crushed cells after centrifugation was used for purification of the Fp00392 protein with Ni-NTA resin and an ultrafiltration centrifuge tube (Beyotime, China). The purified protein was analyzed using 12% SDS-PAGE gels coupled with Coomassie brilliant blue staining.

3. Results

3.1. Identification of the secreted protein Fp00392

The genomic analyses revealed a total of 1,290 secreted proteins in *F. pseudograminearum* (Gardiner *et al.* 2012). However, only a few secreted proteins have been identified in *F. pseudograminearum*, and their functions have not been

thoroughly studied (Gardiner *et al.* 2012; Kazan and Gardiner 2018). The virus-induced virulence effector (VIVE) assay has proven to be an effective means for identifying the virulence effectors from plant pathogens based on whether the effectors can enhance PVX-induced viral symptoms (Shi *et al.* 2020). Initially, we performed a screen to identify the virulence effectors using the VIVE assay. A total of 20 candidate effectors were randomly cloned into the PVX-based expression vector pGR107. *Agrobacterium* strains carrying the PVX-effector constructs were infiltrated into 2-week-old *N. benthamiana* seedlings. About 3 weeks after infiltration, the *N. benthamiana* infiltrated with *Agrobacterium* carrying the PVX-Fp00392 construct showed serious dwarfing with necrosis on the upper leaves, whereas plants infiltrated with *Agrobacterium* carrying the other candidate effectors and negative control GFP showed mild mosaic symptoms (Appendix B). These results indicated that Fp00392 can enhance PVX-induced viral disease symptoms, which suggests that Fp00392 potentially acts as a virulence effector in *F. pseudograminearum*.

With an open reading frame of 441 bp, Fp00392 encodes a protein of 147 amino acids without a known conserved domain. To analyze the phylogenetic distribution of Fp00392 homologues in different pathogens, the protein sequence of Fp00392 was used as a query to Blastp search the NCBI database. Phylogenetic analysis showed that Fp00392 is homologous to VmE02 from *Valsa mali* (GenBank accession no. KUI69068.1), Fg02685 from *F. graminearum* (GenBank accession no. XP_011318636.1) and BFJ71_g10980 from *F. oxysporum* (GenBank accession no. RKK91253.1), which were reported before (Nie *et al.* 2019; Xu *et al.* 2022) (Appendix C). Multiple sequence alignments indicated that these four proteins contain four highly conserved motifs, and Fp00392 is highly homologous to Fg02685 (Appendix D).

3.2. Fp00392 can be secreted into the apoplast

SignalP 4.0 analysis revealed that Fp00392 contains a signal peptide encoded by the first 57 bp. To test whether the predicated signal peptide of Fp00392 functions as a secretory signal, we used a yeast signal trap assay to test for secreted invertase enzymatic activity (Yin *et al.* 2018). The signal peptide sequence of Fp00392 was cloned into the vector pSUC2 to generate pSUC2-Fp00392SP, which was then transformed into the yeast strain YTK12. In the detection assay for invertase enzymatic activity, the yeast YTK12 culture carrying pSUC2-Fp00392SP or pSUC2-Avr1bSP showed a reduction in the conversion of 2,3,5-triphenyltetrazolium chloride (TTC) to insoluble red 1,3,5-triphenylformazan (TPF), whereas the yeast YTK12 culture carrying pSUC2 or pSUC2-Mg87^{N25} and the YTK12 strain culture remained colorless, indicating that the signal peptide of Fp00392 is functional (Fig. 1-A).

To investigate whether Fp00392 is delivered into plant cells during *F. pseudograminearum* infection, the Fp00392-mCherry-NLS construct was generated and transformed into *F. pseudograminearum* using the *A. tumefaciens*-mediated transformation method. The positive transformants were verified by PCR (Appendix E). After wheat coleoptiles were inoculated with the *F. pseudograminearum* strain expressing Fp00392-mCherry-NLS, mCherry signals were observed in the nucleus and cytomembrane of coleoptile cells at the inoculation site (Fig. 1-B). These results revealed that the signal peptide of Fp00392 is functional and delivers the mature protein of Fp00392 into wheat tissues during *F. pseudograminearum* infection.

Considering that functionality, we further investigated the localization of secreted Fp00392 in the plant cells. Fp00392 with or without signal peptide was cloned into vector pCAMBIA1302 to generate pCAMBIA1302:Fp00392-GFP and pCAMBIA1302:Fp00392Δsp-GFP, respectively. These constructs were expressed transiently in *N. benthamiana* leaves *via A. tumefaciens*. After the *N. benthamiana* cells were plasmolyzed, confocal microscopy showed that Fp00392-GFP was mainly localized in the periplasmic spaces and plasma membrane, whereas Fp00392Δsp-GFP was retained in the nucleus, plasma membrane and cytoplasm along with the control GFP (Fig. 1-C).

3.3. Transient expression of Fp00392 triggers cell death in *N. benthamiana*

In the preliminary screening experiment for virulence effectors through the VIVE system, we found that systemic expression of Fp00392 in *N. benthamiana* could trigger necrosis on the upper leaves (Appendix B), which led us to speculate that Fp00392 can induce plant cell death. To further verify where Fp00392 functions, Fp00392 with or without the signal peptide (Fp00392Δsp) was transiently expressed in *N. benthamiana via* agroinfiltration. At 5 days after the infiltration, neither Fp00392Δsp nor the negative control GFP induced cell death, whereas Fp00392 and the positive control INF1 did induce plant cell death (Fig. 2-A). Interestingly, at 7 days after the infiltration, cell death symptoms were observed in the region expressing Fp00392Δsp, while the symptoms of the regions expressing Fp00392, INF1 and GFP remained the same as at 5 days after infiltration (Fig. 2-B). Western blotting confirmed the normal expression of the four genes (Fp00392, Fp00392Δsp, INF1 and GFP) in the infiltrated regions (Fig. 2-C). These results suggested that Fp00392 can function in both intracellular and extracellular spaces of the plant cell, but its localization in the extracellular space accelerates the progress of Fp00392 triggering plant cell death.

3.4. Fp00392 triggers the PTI responses

Because localization in the extracellular space accelerates the progress of Fp00392 triggering plant cell death, and the homologs VmE02 and Fg02685 function as PAMPs, we speculated that Fp00392 also acts as a PAMP. GFP recombinant protein (GFP-His) and Fp00392 recombinant protein (Fp00392-His) were expressed and purified (Fig. 3-A). In the *N. benthamiana* leaves infiltrated with purified Fp00392-His, we detected reactive oxygen species (ROS) accumulation and callose deposition by DAB and trypan blue staining, respectively. As shown in Fig. 3-B, ROS accumulation in the Fp00392-His-infiltrated leaves was much higher than in the leaves infiltrated with negative control GFP-His. Likewise, callose deposition in the Fp00392-His-infiltrated leaves was significantly greater than the leaves infiltrated

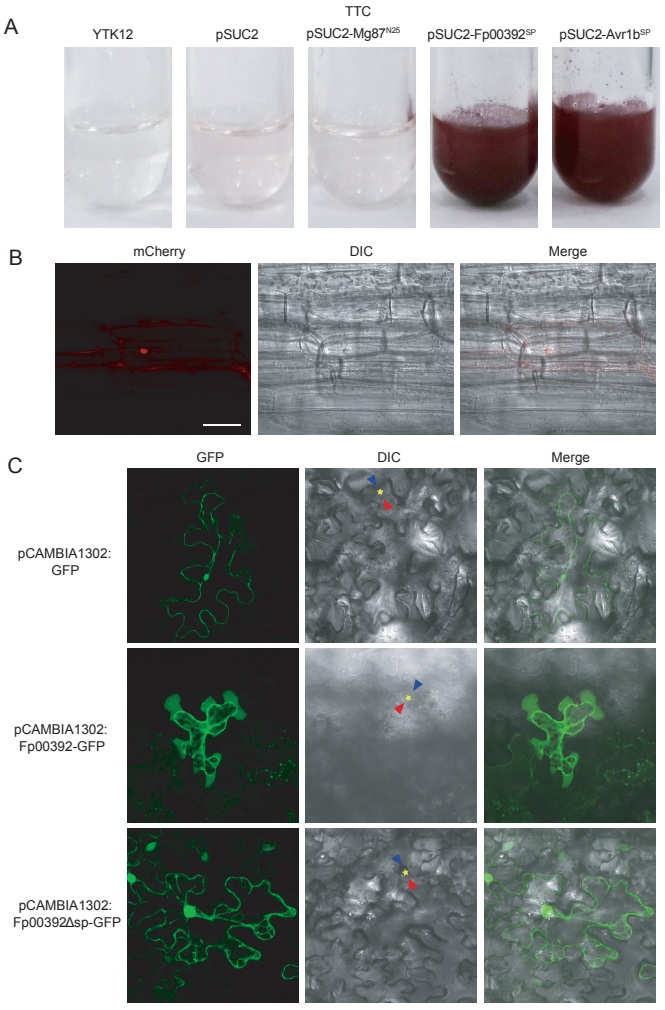


Fig. 1 Fp00392 is a secretory protein from *Fusarium pseudograminearum*. A, functional validation of the signal peptide (SP) of Fp00392 by a yeast invertase secretion system coupled with the detection of invertase enzymatic activity. The yeast YTK12 culture carrying pSUC2-Fp00392SP carried out the reduction of 2,3,5-triphenyltetrazolium chloride (TTC) to the insoluble red 1,3,5-triphenylformazan (TPF). YTK12, untransformed yeast strain; pSUC2-Avr1bSP (the SP of *Phytophthora sojae* effector Avr1b), the positive control; pSUC2 and pSUC2-Mg87^{N25} (the first 25 amino acid residues of the non-secreted Mg87 protein from *Magnaporthe oryzae*), the negative controls. B, mCherry signal observed in the nucleus and cytomembrane of coleoptile cells at the inoculation site during the infection of *F. pseudograminearum* expressing Fp00392-mCherry-NLS. Wheat coleoptiles were inoculated with *F. pseudograminearum* expressing Fp00392-mCherry-NLS, and confocal images were taken at 72 hpi. Bar, 50 μm. C, subcellular localization of Fp00392 in *Nicotiana benthamiana*. Control pCAMBIA1302:GFP, pCAMBIA1302:Fp00392-GFP and pCAMBIA1302:Fp00392Δsp-GFP were transiently expressed in *N. benthamiana* leaves using agroinfiltration. At 48 h after agroinfiltration, leaves were immersed in 0.8 mol L^{-1} mannitol for 20 min to induce plasmolysis, and then samples were observed using a confocal microscope. Yellow asterisks represent the apoplastic spaces between the cell walls (blue arrow) and plasma membranes (red arrow) in plasmolyzed plant cells.

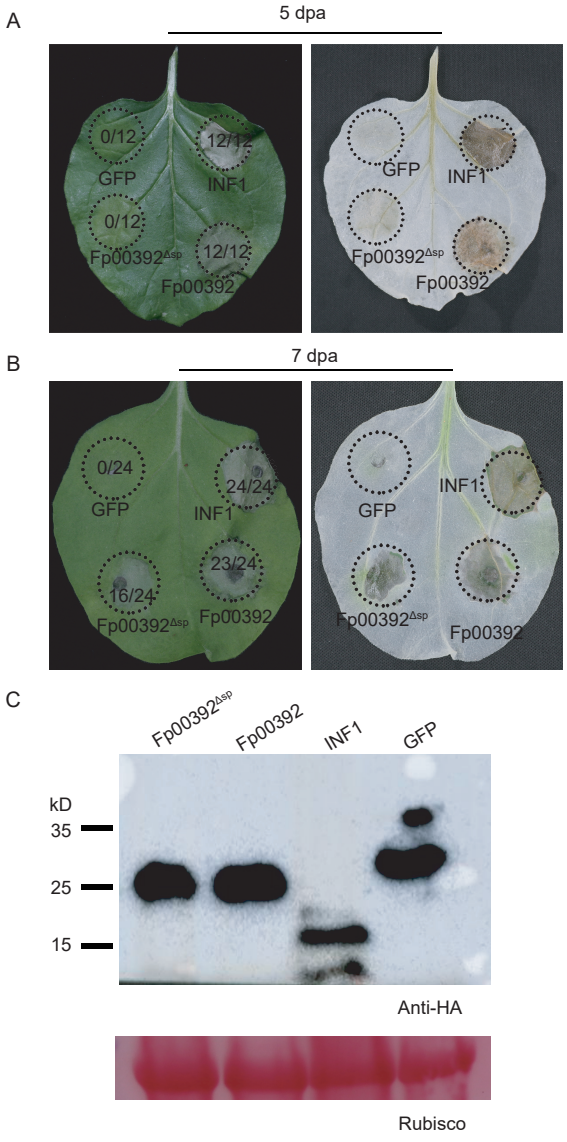


Fig. 2 Localization in the extracellular space accelerates the progress of Fp00392 triggering plant cell death. A and B, phenotypes of *Nicotiana benthamiana* expressing Fp00392 and Fp00392 without the signal peptide (Fp00392Δsp) at 5 and 7 days post agroinfiltration (dpa). GFP and INF1 were used as the negative and positive controls, respectively. C, immunoblot analysis of proteins from *N. benthamiana* expressing Fp00392, Fp00392Δsp, GFP and INF1 fused with 3×HA tags.

with negative control GFP-His (Fig. 3-C). In addition, to further confirm whether Fp00392 activates plant immunity responses during the induction of cell death, the transcript levels of immunity-related marker genes were analyzed in the *N. benthamiana* leaves. As shown in Appendix F-a, the transcript levels of two defense marker genes (*NbPR1a* and *NbPR2*) and two hypersensitive response-specific genes (*NbHIN1* and *NbHSR203J*) were notably increased in the *N. benthamiana* leaves infiltrated with Fp00392-His compared with the leaves infiltrated with negative control GFP-His. Simultaneously, several PTI-related marker genes in the *N. benthamiana* leaves were also examined. The qRT-PCR data showed that the transcript levels of *NbCYP71D20*, *NbACRE31*, *NbPTI5* and *NbWRKY7* were subsequently increased in the *N. benthamiana* leaves infiltrated with Fp00392-His compared with the leaves infiltrated with negative control GFP-His (Appendix F-b). These results clearly demonstrate that Fp00392 is an active PAMP.

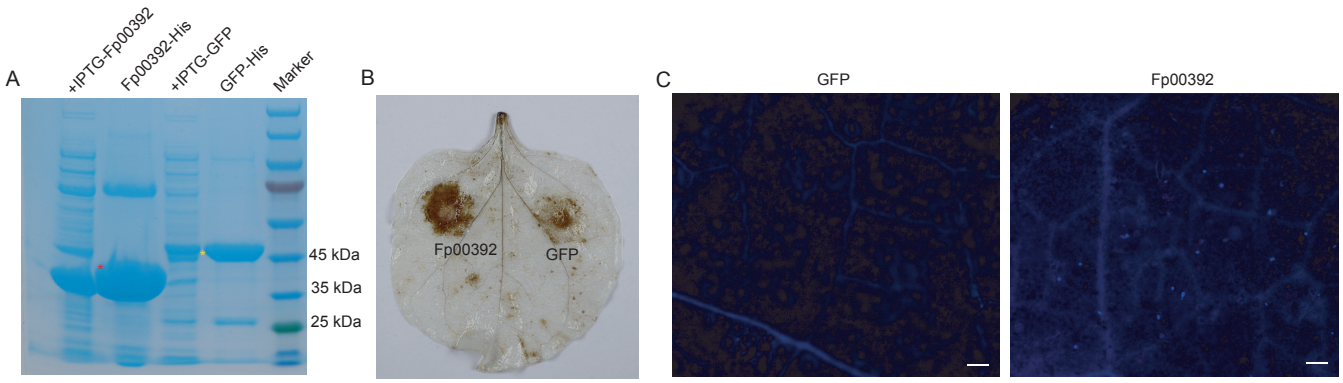


Fig. 3 Fp00392 triggers immunity responses in *Nicotiana benthamiana*. A, SDS-PAGE analysis of recombinant protein Fp00392-His and GFP-His purified from *Escherichia coli*. The first and third lanes are the soluble protein extracts of the *E. coli* carrying Fp00392-His and GFP-His with induction by IPTG, respectively. The second and fourth lanes show purified recombinant protein Fp00392-His and GFP-His. The red asterisk represents objective protein Fp00392-His, and the yellow asterisk represents objective protein GFP-His. B and C, accumulation of reactive oxygen species (ROS) and callose. *Nicotiana benthamiana* leaves were infiltrated with 1 μmol L^{-1} of purified protein Fp00392-His or GFP-His. After 24 h, the leaves were sampled. For ROS accumulation (B), samples were stained with DAB, followed by decolorization with ethanol. For callose deposition (C), samples were stained with aniline blue, followed by bleaching with ethanol. Bar, are 20 μm.

3.5. BAK1 and SOBIR1 do not mediate Fp00392-triggered cell death in *N. benthamiana*

Considering that BAK1 and SOBIR1 usually serve as co-receptors for numerous PRRs in plants, which are required for cell death triggered by the homolog VmE02 of Fp00392, we investigated whether the ability of Fp00392 to trigger plant immunity depends on the two co-receptors BAK1 and SOBIR1. The virus-induced gene silencing (VIGS) assay mediated by tobacco rattle virus (TRV) was employed to generate *NbBAK1*- and *NbSOBIR1*-silenced *N. benthamiana* plants (Appendix G-a). An obvious photo-bleaching phenotype was observed in the *NbPDS*-silenced plants (Appendix G-a), indicating that the TRV-VIGS system functioned effectively. qRT-PCR analysis showed that the transcript levels of *NbBAK1* and *NbSOBIR1* were significantly reduced in *NbBAK1*- and *NbSOBIR1*-silenced *N. benthamiana* plants, respectively (Appendix G-b). Subsequently, *NbBAK1*-, *NbSOBIR1*- and the negative control *GFP*-silenced *N. benthamiana* plants were infiltrated with *Agrobacterium* carrying the PVX-INF1 and PVX-Fp00392 constructs. As shown in Appendix G-c, positive control INF1 did not trigger cell death in the leaves of *NbBAK1*- and *NbSOBIR1*-silenced *N. benthamiana* plants, whereas Fp00392 was still able to trigger cell death in the leaves of *NbBAK1*-, *NbSOBIR1*- and negative control *GFP*-silenced *N. benthamiana* plants. Western blotting confirmed the normal expression of genes Fp00392 and INF1 in the infiltrated regions (Appendix G-d). These results indicate that Fp00392-triggered plant cell death is independent of the two co-receptors BAK1 and SOBIR1.

3.6. Fp00392 is highly expressed during *F. pseudograminearum* infection

To explore the potential contribution of Fp00392 to *F. pseudograminearum* virulence, the expression pattern of *Fp00392* during the infection process of *F. pseudograminearum* was analyzed firstly. The qRT-PCR assay showed that the transcript levels of *Fp00392* gradually increased during the early stages of *F. pseudograminearum* infection (12, 24, 36 hpi), continued to increase to a peak (approximately 250-fold) at 48 hpi, and then diminished thereafter (Fig. 4). The qRT-PCR results clearly indicate that the transcript levels of *Fp00392* were up-regulated, suggesting that it plays an important role in *F. pseudograminearum* infection.

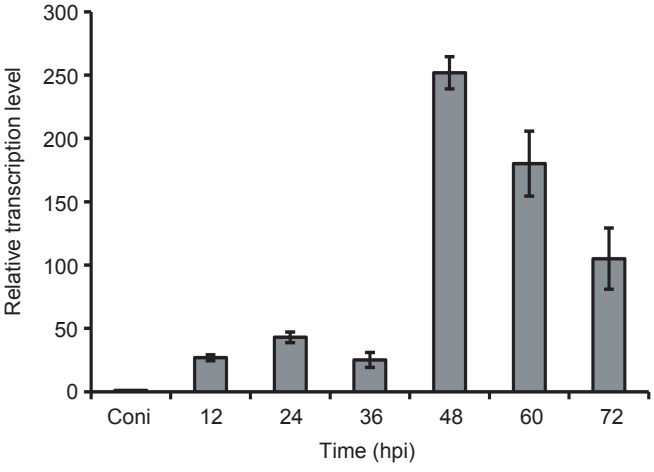


Fig. 4 Relative transcript levels of *Fp00392* at different *Fusarium pseudograminearum* infection stages. Wheat coleoptiles (Xinong 979) inoculated with fresh conidium of wild-type strain (HNAY190416) were sampled at different time points according to the infection stage of *F. pseudograminearum*. Conidium (Coni) was used as a control. Relative transcript levels of *Fp00392* were calculated by the comparative threshold ($2^{-\Delta\Delta CT}$) method. The quantitative RT-PCR values were normalized to the transcript level of the *F. pseudograminearum Tubulin* gene. Values represent the mean±standard deviation of three independent biological samples. The transcript level of *Fp00392* during *F. pseudograminearum* infection stages at the Coni stage was standardized to 1. hpi, hours post inoculation.

3.7. Fp00392 is required for the virulence of *F. pseudograminearum* in wheat

To more directly confirm the important role of Fp00392 during *F. pseudograminearum* infection, deletion mutants and complemented transformants of *Fp00392* in *F. pseudograminearum* were constructed and verified by PCR or Southern blotting (Appendices H and I). Subsequently, we evaluated the pathogenicity of the Δ*Fp00392-12* mutant, wild-type strain and complemented transformants on wheat coleoptile. Inoculation assays showed that the lesion length on wheat coleoptiles inoculated with the Δ*Fp00392-12* mutant was significantly shorter than that on wheat coleoptiles inoculated with the wild-type strain at 10 dpi, whereas the complemented transformants largely restored *F. pseudograminearum* virulence to wheat coleoptiles (Fig. 5-A). The relative *F. pseudograminearum* biomass confirmed a reduction in wheat coleoptiles inoculated with Δ*Fp00392-12* mutant compared with the wild-type strain and complemented transformants (Fig. 5-B). These results indicated that Fp00392 contributes to the pathogenicity of *F. pseudograminearum* on wheat coleoptiles.

3.8. Effect of *Fp00392* deletion on the tolerance of *F. pseudograminearum* to H_2O_2 and Congo Red

To investigate that whether *Fp00392* is involved in the response of *F. pseudograminearum* to environmental stress, we analyzed the growth of wild-type strain, Δ*Fp00392-12* mutant and complemented transformants under different environmental stress conditions. First, we found that the Δ*Fp00392-12* mutant showed a filamentous growth rate and colony morphology similar to the wild-type strain and complemented transformants on PDA medium (Fig. 6-A and B), suggesting that Fp00392 does not participate in the mycelia growth process of *F. pseudograminearum*. Subsequently, the growth of the above three strains on PDA medium containing either 2 mg mL^{-1} Congo Red or 20 mmol L^{-1} H_2O_2 was analyzed. The relative inhibition rate of the Δ*Fp00392-12* mutant was significantly lower than those of wild-type strain and complemented transformants on PDA medium containing 20 mmol L^{-1} H_2O_2 or 2 mg mL^{-1} Congo Red after culturing for 3 days (Fig. 6-A and B). Interestingly, the hyphal density of the Δ*Fp00392-12* mutant was conspicuously sparse compared to those of the wild-type strain and complemented transformants on PDA medium containing 2 mg mL^{-1} Congo Red. These results suggested that the deletion of *Fp00392* improves the tolerance of *F. pseudograminearum* to oxidative stress, but may weaken the tolerance of *F. pseudograminearum* to Congo Red.

4. Discussion

Apoplastic secreted proteins play an important role in plant–pathogen interactions. Many of these apoplastic secreted proteins can be perceived by plant PRRs as PAMPs to trigger plant innate immune responses (Kamoun 2006; Qutob *et al.* 2006). In this study, we identified the apoplastic secreted protein Fp00392, which is not only perceived as a PAMP to trigger the plant immune response but acts as a crucial virulence factor for *F. pseudograminearum* infection in wheat.

Sequence analysis showed that Fp00392 is homologous to VmE02 from *Valsa mali* and Fg02685 from *F. graminearum*, which have been reported before and shown to function as PAMPs (Nie *et al.* 2019; Xu *et al.* 2022). Like VmE02 and Fg02685，Fp00392 can trigger cell death in *N. benthamiana* (Fig. 2), suggesting that Fp00392 functions as a PAMP. As expected, Fp00392 displays the typical characteristics of PAMPs, including the stimulation of ROS accumulation and callose deposition (Fig. 3). PTI defenses triggered by PAMPs also include transcriptional activation of some defense-related genes, such as *CYP71D20*, *PR1a*, *ERF1* and others (Dean

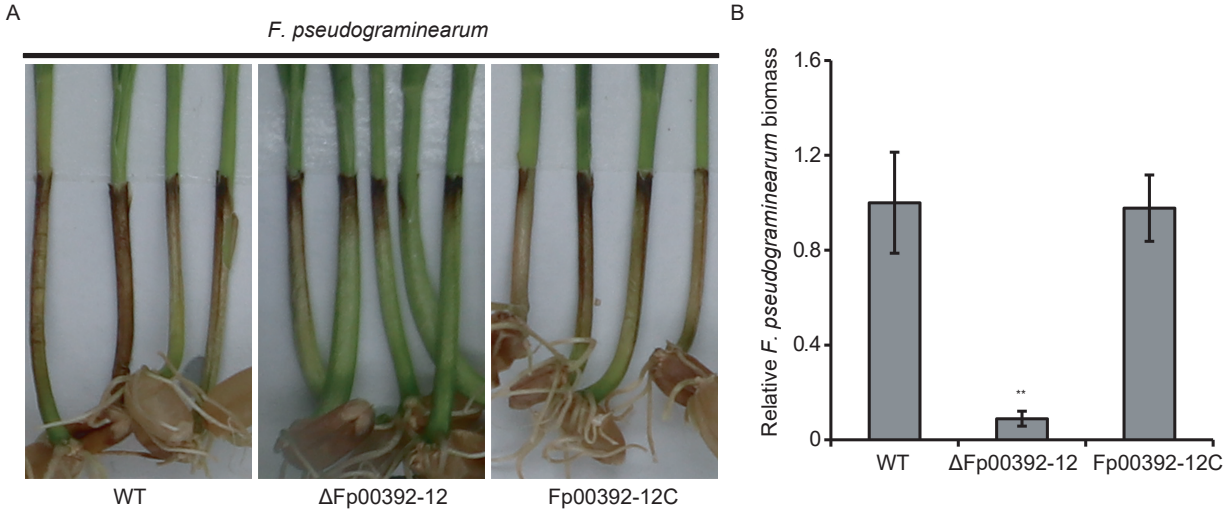


Fig. 5 *Fp00392* is required for the virulence of *Fusarium pseudograminearum* in wheat. A, symptoms of wheat coleoptiles inoculated with *F. pseudograminearum* wild type, the knockout mutant Δ*Fp00392-12* and the complemented strain *Fp00392-12C* at 10 days post inoculation (dpi). B, analysis of *F. pseudograminearum* biomass in wheat coleoptiles at 10 dpi by genomic DNA (gDNA)-based qPCR. Values represent the mean±standard deviation of three independent biological samples. Differences were assessed using Student's *t*-tests. **, $P<0.01$.

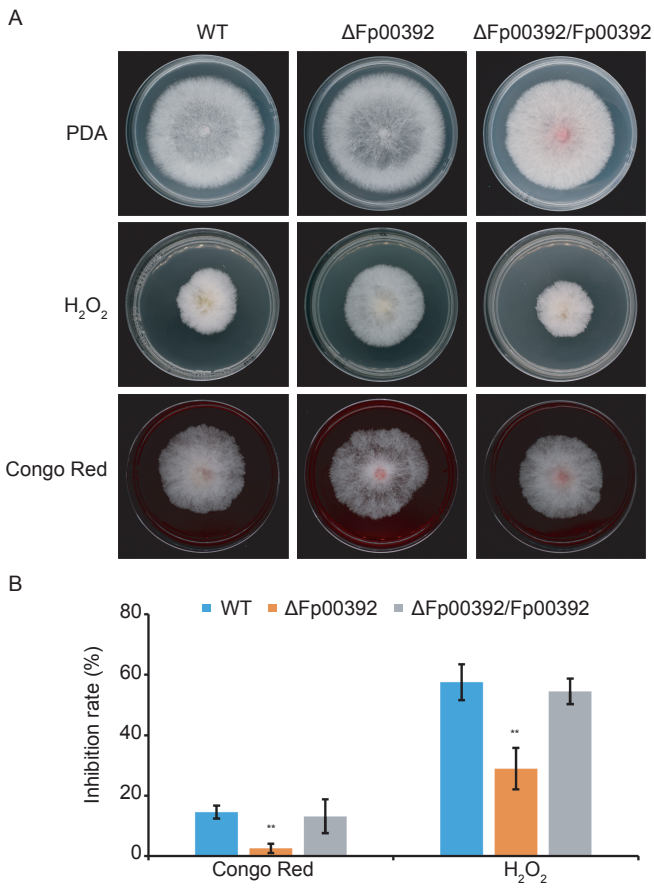


Fig. 6 Deletion of Fp00392 affects the sensitivity of *Fusarium pseudograminearum* to H_2O_2 and Congo Red. A, phenotypes of *F. pseudograminearum* wild type, the knockout mutant Δ*Fp00392-12* and the complemented strain *Fp00392-12C* grown on potato dextrose agar (PDA) and PDA with the indicated stress agents at 3 days post inoculation (dpi). B, statistical analysis of the relative inhibition rates (%) of wild type, ΔFp00392-12 and Fp00392-12C. H_2O_2, hydrogen peroxide. Values represent the mean±standard deviation (SD) with ten replicates. The statistical analyses of experimental groups comparing to controls were evaluated by Student's *t*-test (**, $P<0.01$).

et al. 2005; Heese *et al.* 2007; Dou and Zhou 2012). Our data showed that Fp00392 can induce the up-regulation of several defense-related genes in *N. benthamiana* (Appendix F). Many PAMPs, such as INF1, VmE02, XEG1, SGP1 and others, function in the apoplast of plants (Kamoun *et al.* 1998; Ma *et al.* 2015; Nie *et al.* 2019; Song *et al.* 2021). Like other PAMPs, Fp00392 is mainly localized in the apoplast of *N. benthamiana* (Fig. 1-C), and the signal peptide is important for plant cell death induced by Fp00392 (Fig. 2), implying that Fp00392 functions in the apoplast of plants. Taken together, these results reveal that Fp00392 functions as a PAMP.

In addition to activating the immune response, many PAMPs have been reported as virulence factors. For example, deletion of VmE02 and Fg02685, which are homologs of Fp00392, reduced the virulence of *V. mali* and *F. graminearum*, respectively (Nie *et al.* 2019; Xu *et al.* 2022); and silencing both SGP1 and *UvGHF1* in *U. virens* reduced the number of false smut balls per panicle (Song *et al.* 2021; Zou *et al.* 2023). As in these examples, Fp00392 is an important virulence factor in *F. pseudograminearum*, as evidenced by the up-regulated expression of Fp00392 during infection with *F. pseudograminearum* and the reduced pathogenicity of deletion mutants of Fp00392 in *F. pseudograminearum* (Figs. 4 and 5). Therefore, it is very interesting to investigate how *F. pseudograminearum* coordinates the two opposing functions of Fp00392, namely the virulence function and induction of the immune response, during infection with *F. pseudograminearum*. Pathogens are known to secrete numerous effectors during infection, some of which can inhibit the PTI response of plants. Therefore, one strong possibility is that although Fp00392 can induce the immune response, that induced immune response may be suppressed by other effectors secreted from *F. pseudograminearum* to facilitate the pathogenic infection.

Tolerance to oxidative stress is important for plant pathogens, and the degree of tolerance may be associated with pathogenicity during host infection (Heller and Tudzynski 2011; Segal and Wilson 2018). In this study, the deletion of Fp00392 results in greater oxidative stress tolerance in *F. pseudograminearum* (Fig. 6-A and B), which should mean that deletion of Fp00392 leads to increased pathogenicity of *F. pseudograminearum* in theory. However, we found that the deletion of Fp00392 weakened the virulence of *F. pseudograminearum* in wheat (Fig. 5). We speculate that Fp00392 may function independently in oxidative stress tolerance and virulence of *F. pseudograminearum*. During Δ*Fp00392* mutant infection, the Δ*Fp00392* mutant can be resistant to oxidative stress produced by plants, but it may have growth defects, which may result in the deletion of Fp00392 weakening the virulence of *F. pseudograminearum* in wheat. There is insufficient evidence that the deletion of *Fp00392* causes defects in the growth of *F. pseudograminearum*, and this possibility will be studied in the future.

PAMPs are recognized by PRRs and hence trigger PTI. In most cases, receptor-associated kinases BAK1 and SOBIR1 act as co-receptors of PRRs for transmitting signals from the perception of PAMPs (Heese *et al.* 2007). For instance, RXEG1 and RE02, which recognize XEG1 from *P. sojae* and VmE02 from *V. mali*, respectively, recruit BAK1 and SOBIR1 to form a receptor complex that can transduce defense signals upon binding to XEG1 and VmE02, respectively (Wang *et al.* 2018; Nie *et al.* 2021). However, at least some PAMPs do not require BAK1 for triggering PTI. For example, chitin from fungi can recognize and directly bind to LysMs in the ectodomain of receptor kinase CERK1 to trigger CERK1 phosphorylation and the subsequent immune signal (Liu T T *et al.* 2012). Like Fg02658, the Fp00392-triggered immune response is independent of the two co-receptors BAK1 and SOBIR1 (Appendix G). Presumably, Fp00392 may recognize and bind directly to regions in the ectodomain of some protein(s) located in the membrane of plant cells.

In summary, the results of this study revealed that a secreted protein from *F. pseudograminearum,* Fp00392, induces the immune response in plants. Future studies will focus on exploring the receptors recognized by Fp00392 to further reveal how it activates the immune response.

5. Conclusion

We identified a PAMP from *F. pseudograminearum*, Fp00392, that triggers cell death in *N. benthamiana*. Fp00392 can activate the ROS burst, callose deposition, and the up-regulation of defense-related genes in *N. benthamiana*. In addition, Fp00392-triggered cell death is independent of BAK1 and SOBIR1. Further analyses showed that Fp00392 is required for the virulence of *F. pseudograminearum* in wheat. The identification and functional characterization of Fp00392 are important for our understanding of how Fp00392 regulates the plant immune response and contributes to the virulence of *F. pseudograminearum* in wheat.

Acknowledgements

This study was supported by the National Natural Science Foundation of China (32102153), the Natural Science Foundation of Anhui Higher Education Institutions, China (2023AH040139) and the Talent Research Project of Anhui Agricultural University, China (rc342218).

Declaration of competing interest

The authors declare that they have no conflict of interest.

Declaration of generative AI and AI-assisted technologies in the writing process

The authors declare that they did not use AI in the preparation and writing of this manuscript.

Appendices associated with this paper are available at https://doi.org/10.1016/j.jia.2025.02.030

References

Akinsanmi O, Mitter V, Simpfendorfer S, Backhouse D, Chakraborty S. 2004. Identity and pathogenicity of *Fusarium* spp. isolated from wheat fields in Queensland and northern New South Wales. *Australian Journal of Agricultural Research*, **55**, 97–107.

Brunner F. 2014. Pep-13, a plant defense-inducing pathogen-associated pattern from *Phytophthora* transglutaminases. *EMBO Journal*, **21**, 6681–6688.

Chakraborty D S, Liu C J, Mitter V, Simpfendorfer S. 2006. Pathogen population structure and epidemiology are keys to wheat crown rot and Fusarium head blight management. *Australasian Plant Pathology*, **35**, 1–113.

Dean J D, Goodwin P H, Hsiang T. 2005. Induction of glutathione S-transferase genes of *Nicotiana benthamiana* following infection by *Colletotrichum destructivum* and *C. orbiculare* and involvement of one in resistance. *Journal of Experimental Botany*, **56**, 1525–1533.

Dou D L, Zhou J M. 2012. Phytopathogen effectors subverting host immunity: Different foes, similar battleground. *Cell Host Microbe*, **12**, 484–495.

Felix G, Duran J D, Volko S, Boller T. 1999. Plants have a sensitive perception system for the most conserved domain of bacterial flagellin. *Plant Journal*, **18**, 265–276.

Gardiner D M, McDonald M C, Covarelli L, Solomon P S, Rusu A G, Marshall M, Kazan K, Chakraborty S, McDonald B A, Manners J M. 2012. Comparative pathogenomics reveals horizontally acquired novel virulence genes in fungi infecting cereal hosts. *PLoS Pathogens*, **8**, e1002952.

Gust A A, Biswas R, Lenz H D, Rauhut T, Ranf S, Kemmerling B, G€otz F, Glawischnig E, Lee J, Felix G. 2007. Bacteria-derived peptidoglycans constitute pathogen-associated molecular patterns triggering innate immunity in *Arabidopsis*. *Journal of Biological Chemistry*, **282**, 32338–32348.

Heese A, Hann D R, Gimenez-Ibanez S, Jones A M, He K, Li J, Schroeder J I, Peck S C, Rathjen J P. 2007. The receptor-like kinase SERK3/BAK1 is a central regulator of innate immunity in plants. *Proceedings of the National Academy of Sciences of the United States of America*, **104**, 12217–12222.

Heller J, Tudzynski P. 2011. Reactive oxygen species in phytopathogenic fungi: Signaling, development and disease. *Annual Review of Phytopathology*, **49**, 369–390.

Ji L J, Kong L X, Li Q S, Wang L S, Chen D, Ma P. 2016. First report of *Fusarium pseudograminearum* causing Fusarium Head Blight of wheat in Hebei Province, China. *Plant Disease*, **100**, 220.

Jones J D, Dangl J L. 2006. The plant immune system. *Nature*, **444**, 323−329.

Kamoun S. 2006. A catalogue of the effector secretome of plant pathogenic oomycetes. *Annual Review of Phytopathology*, **44**, 41–60.

Kamoun S, van West P, Vleeshouwers V G, de Groot K E, Govers F. 1998. Resistance of *Nicotiana benthamiana* to *Phytophthora infestans* is mediated by the recognition of the elicitor protein INF1. *Plant Cell*, **10**, 1413–1426.

Kang J B, Zhang J, Liu Y K, Song J C, Ou J L, Tao X, Zhou M G, Duan Y B. 2023. Mitochondrial dynamics caused by QoIs and SDHIs fungicides depended on FgDnm1 in *Fusarium graminearum*. *Journal of Integrative Agriculture*, **22**, 481–494.

Kazan K, Gardiner D M. 2018. Fusarium crown rot caused by *Fusarium pseudograminearum* in cereal crops: Recent progress and future prospects. *Molecular Plant Pathology*, **19**, 1547–1562.

Kunze G, Zipfel C, Robatzek S, Niehaus K, Boller T, Felix G. 2004. The N terminus of bacterial elongation factor Tu elicits innate immunity in *Arabidopsis* plants. *Plant Cell*, **16**, 3496–3507.

Li H L, Yuan H X, Fu B, Xing X P, Sun B J, Tang W H. 2012. First report of *Fusarium pseudograminearum* causing crown rot of wheat in Henan, China. *Plant Disease*, **96**, 1065.

Liu B, Li J F, Ao Y, Qu J, Wang H B. 2012. Lysin motif-containing proteins LYP4 and LYP6 play dual roles in peptidoglycan and chitin perception in rice innate immunity. *Plant Cell*, **24**, 3406–3419.

Liu S M, Duan Y B, Ge C Y, Chen C J, Zhou M G. 2013. Functional analysis of the β2-tubulin gene of *Fusarium graminearum* and the β-tubulin gene of *Botrytis cinerea* by homologous replacement. *Pest Management Science*, **69**, 582–588.

Liu T T, Liu Z X, Song C J, Hu Y F, Han Z F, She J, Fan F F, Wang J W, Jin C W, Chang J B, Zhou J M, Chai J J. 2012. Chitin-induced dimerization activates a plant immune receptor. *Science*, **336**, 1160–1164.

Livak K, Schmittgen T. 2001. Analysis of relative gene expression data using Real-Time quantitative PCR and the $2^{-\Delta\Delta CT}$ method. *Methods*, **25**, 402–408.

Ma Z C, Song T Q, Zhu L, Ye W W, Wang Y, Shao Y Y, Dong S M, Zhang Z G, Dou D L, Zheng X B, Tyler B M, Wang Y C. 2015. A *Phytophthora sojae* glycoside hydrolase 12 protein is a major virulence factor during soybean infection and is recognized as a PAMP. *Plant Cell*, **27**, 2057–2072.

Monds R D, Cromey M G, Lauren D R, di Menna M, Marshall J. 2005. *Fusarium graminearum*, *F. cortaderiae* and *F. pseudograminearum* in New Zealand: Molecular phylogenetic analysis, mycotoxin chemotypes and co-existence of species. *Mycological Research*, **109**, 410–420.

Nie J J, Yin Z Y, Li Z P, Wu Y X, Huang L L. 2019. A small cysteine-rich protein from two kingdoms of microbes is recognized as a novel pathogen-associated molecular pattern. *New Phytologist*, **222**, 995–1011.

Nie J J, Zhou W J, Liu J Y, Tan N, Zhou J M, Huang L L. 2021. A receptor-like protein from *Nicotiana benthamiana* mediates VmE02 PAMP-triggered immunity. *New Phytologist*, **229**, 2260–2272.

Obanor F, Chakraborty S. 2014. Aetiology and toxigenicity of *Fusarium graminearum* and *F. pseudograminearum* causing crown rot and head blight in Australia under natural and artificial infection. *Plant Pathology*, **63**, 1218–1229.

Qutob D, Kemmerling B, Brunner F, Küfner I, Engelhardt S, Gust A A, Luberacki B, Seitz H U, Stahl D, Rauhut T, Glawischnig E, Schween G, Lacombe B, Watanabe N, Lam E, Schlichting R, Scheel D, Nau K, Dodt G, Hubert D, *et al.* 2006. Phytotoxicity and innate immune responses induced by Nep1-like proteins. *Plant Cell*, **18**, 3721–3744.

Ranf S, Gisch N, Schäffer M, Illig T, Westphal L, Knirel Y A, Sánchez-Carballo P M, Zähringer U, Hückelhoven R, Lee J, Scheel D. 2015. A lectin S-domain receptor kinase mediates lipopolysaccharide

sensing in *Arabidopsis thaliana*. *Nature Immunology*, **16**, 426–433.
Ron M, Avni A. 2004. The receptor for the fungal elicitor ethylene-inducing xylanase is a member of a resistance-like gene family in tomato. *Plant Cell*, **16**, 1604–1615.
Rotblat B, Enshell-Seijffers D, Gershoni J M, Schuster S, Avni A. 2002. Identification of an essential component of the elicitation active site of the EIX protein elicitor. *Plant Journal*, **32**, 1049–1055.
Segal L M, Wilson R A. 2018. Reactive oxygen species metabolism and plant-fungal interactions. *Fungal Genetics and Biology*, **110**, 1–9.
Shi J X, Zhu Y H, Li M, Ma Y Q, Liu H R, Zhang P, Fang D, Guo Y S, Xu P, Qiao Y L. 2020. Establishment of a novel virus-induced virulence effector assay for the identification of virulence effectors of plant pathogens using a PVX-based expression vector. *Molecular Plant Pathology*, **21**, 1654–1661.
Shinya T, Nakagawa T, Kaku H, Shibuya N. 2015. Chitin-mediated plant fungal interactions: Catching, hiding and handshaking. *Current Opinion in Plant Biology*, **26**, 64–71.
Song T Q, Zhang Y, Zhang Q, Zhang X, Shen D Y, Yu J J, Yu M N, Pan X Y, Cao H J, Yong M L, Qi Z Q, Du Y, Zhang R S, Yin X L, Qiao J Q, Liu Y Z, Liu W D, Sun W X, Zhang Z G, Wang Y C, *et al.* 2021. The N-terminus of an *Ustilaginoidea virens* Ser-Thr-rich glycosylphosphatidylinositol-anchored protein elicits plant immunity as a MAMP. *Nature Communication*, **12**, 2451.
Wang J X, Liu S, Ren P, Jia F G, Kang F, Wang R L, Xue R Z, Yan X, Huang L L. 2023. A novel protein elicitor (PeSy1) from *Saccharothrix yanglingensis* induces plant resistance and interacts with a receptor-like cytoplasmic kinase in *Nicotiana benthamiana*. *Molecular Plant Pathology*, **24**, 436–451.
Wang Y, Xu Y P, Sun Y J, Wang H B, Qi J M, Wan B W, Ye W W, Lin Y C, Shao Y Y, Dong S M, Tyler B M, Wang Y C. 2018. Leucine-rich repeat receptor-like gene screen reveals that *Nicotiana* RXEG1 regulates glycoside hydrolase 12 MAMP detection. *Nature Communication*, **9**, 594.
Xu F, Song Y L, Yang G Q, Wang J M, Liu L L, Li Y H. 2015. First report of *Fusarium pseudograminearum* from wheat heads with Fusarium head blight in North China plain. *Plant Disease*, **99**, 156.
Xu Q, Hu S, Jin M X, Xu Y J, Jiang Q T, Ma J, Zhang Y Z, Qi P F, Chen G Y, Jiang Y F, Zheng Y L, Wei Y M. 2022. The N-terminus of a *Fusarium graminearum*-secreted protein enhances broad-spectrum disease resistance in plants. *Molecular Plant Pathology*, **23**, 1751–1764.
Yin W X, Wang Y F, Chen T, Lin Y, Luo C X. 2018. Functional evaluation of the signal peptides of secreted proteins. *Bio-Protocol*, **8**, e2839.
Zhang X W, Jia L J, Zhang Y, Jiang G, Li X, Zhang D, Tang W H. 2012. In planta stage-specific fungal gene profiling elucidates the molecular strategies of *Fusarium graminearum* growing inside wheat coleoptiles. *Plant Cell*, **24**, 5159–5176.
Zhang X X, Sun H Y, Shen C M, Li W, Chen H G. 2015. Survey of Fusarium spp. causing wheat crown rot in major winter wheat growing regions of China. *Plant Disease*, **99**, 1610–1615.
Zipfel C. 2014. Plant pattern-recognition receptors. *Trends in Immunol*, **35**, 345–351.
Zou J Y, Jiang C Q, Qiu S S, Duan G H, Wang G Q, Li D Y, Yu S W, Zhao D, Sun W X. 2023. An *Ustilaginoidea virens* glycoside hydrolase 42 protein is an essential virulence factor and elicits plant immunity as a PAMP. *Molecular Plant Pathology*, **24**, 1414–1429.

Executive Editor-in-Chief Fanghao Wan
Managing Editor Juan Zhang